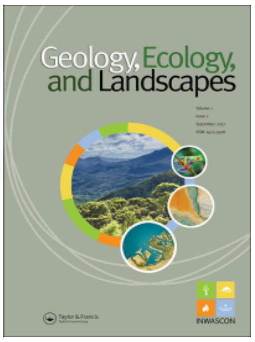

Geology, Ecology, and Landscapes

ISSN: 2474-9508 (Online) Journal homepage: www.tandfonline.com/journals/tgel20

Biocompatible graphite-coated electrodes for sustainable plant-based energy harvesting

Sk Rakibur Rahman, Eng-Eng Ngu, Gwo-Chin Chung, Wai-Leong Pang, Kar Ban Tan, Ajay Kumar Singh, Muhammad Aqeel Ashraf & Kah-Yoong Chan

To cite this article: Sk Rakibur Rahman, Eng-Eng Ngu, Gwo-Chin Chung, Wai-Leong Pang, Kar Ban Tan, Ajay Kumar Singh, Muhammad Aqeel Ashraf & Kah-Yoong Chan (08 Mar 2026): Biocompatible graphite-coated electrodes for sustainable plant-based energy harvesting, Geology, Ecology, and Landscapes, DOI: 10.1080/24749508.2026.2640713

To link to this article: https://doi.org/10.1080/24749508.2026.2640713

Published online: 08 Mar 2026.

GEOLOGY, ECOLOGY, AND LANDSCAPES
https://doi.org/10.1080/24749508.2026.2640713

RESEARCH ARTICLE

OPEN ACCESS Check for updates

Biocompatible graphite-coated electrodes for sustainable plant-based energy harvesting

Sk Rakibur Rahman[a], Eng-Eng Ngu[a,b], Gwo-Chin Chung[a], Wai-Leong Pang[c], Kar Ban Tan[d], Ajay Kumar Singh[e], Muhammad Aqeel Ashraf[a] and Kah-Yoong Chan[a,f]

[a]Faculty of Artificial Intelligence and Engineering, Multimedia University, Cyberjaya, Malaysia; [b]Centre for Electric Energy and High Voltage Engineering, COE for Robotics and Sensing Technologies, Multimedia University, Cyberjaya, Malaysia; [c]School of Engineering, Faculty of Innovation & Technology, Taylor's University, Subang Jaya, Malaysia; [d]Department of Chemistry, Faculty of Science, Universiti Putra Malaysia, Serdang, Malaysia; [e]Faculty of Electronics and Communication Engineering, NIIT University, Neemrana, India; [f]Centre for Advanced Devices and Systems, COE for Robotics and Sensing Technologies, Multimedia University, Cyberjaya, Malaysia

ABSTRACT

The environmental effects of fossil fuel consumption have continued to promote research in other energy sources that are more eco-friendly and can be sustained in the long run. One of the promising energy harvesting methods is plant-based energy harvesting, which has been considered a potential approach in developing energy harvesting systems for low-power applications, such as precision agriculture, environmental monitoring, and IoT sensor networks. The present research aimed to evaluate the potential of long-term energy harvesting using an *Aloe vera* plant, considering its health and the biocompatibility of electrodes. There was a challenge when uncoated zinc *(Zn)* and copper *(Cu)* electrodes emitted toxic ions (Zn^{2+} and Cu^{2+}) that initiated foliar desiccation, tissue necrosis, and physiological degradation. Graphite-coated electrodes were henceforth brought in as biocompatible alternatives for reducing ion leakage while maintaining electrical conductivity. A commercially used wound-healing agent was also applied at sites of electrode insertion to facilitate tissue conservation. The health of the plants and energy harvesting were monitored over a period of 7 days. The results of this research have shown that material modification and application of a wound-healing agent have a positive effect on plant health without compromising energy harvesting.

ARTICLE HISTORY
Received 3 November 2025
Accepted 2 March 2026

KEYWORDS
PBC; graphite coating; plant-based energy; IoT; ion leakage

1. Introduction

The current world energy deficit can be attributed primarily to an ongoing reliance on finite fossil fuels, rapidly increasing energy demand, and environmental concerns related to global warming (Gitelman & Kozhevnikov, 2023). As oil, coal, and natural gas reserves dwindle, competition for the remaining resources is heating up, leading to continued price volatility and supply uncertainty (Cherp et al., 2021). Even more so, coal, natural gas, and oil make up over 75% of worldwide greenhouse gas emissions, which contribute to climate change and increase the occurrence of extreme weather (Intergovernmental Panel on Climate Change [IPCC], 2023). Thus, considerations on sustainable energy options are necessary to avert a repeat of energy insecurity and environmental pollution in the future.

Because of the energy crunch, renewable sources of energy (solar, wind, hydro, and biofuels) are important, as they are the renewable and dirtier end of carbon emissions (Haegel et al., 2019). With improved investments and policies, research indicates that renewable energy can supply 90% of the world's electricity by 2050 (Jacobson et al., 2019). The prices of solar and wind energy have fallen, allowing them to compete with prices for fossil fuels (Shukor et al., 2023; Victoria et al., 2021; Yeoh & Chan, 2017, 2021). Small-scale renewable energy systems improve access to energy and reduce energy poverty in developing countries (Stritzke & Jain, 2021; Tan & Chan, 2024). Emerging DC–DC converters can also exploit multiple renewable energy resources to enhance conversion efficiency and to reduce the complexity of the energy harvesting system (Choong & May, 2023).

Local mechanical vibrations are used to produce energy in conjunction with conventional renewable sources. Triboelectric nanogenerators (TENGs) have undergone substantial investigation for low-power sensing and wearable applications (Feng et al., 2019). They produce electrical signals by mechanical contact and vibrations. Flexible, hydrogel-based structures that improve ionic conductivity may be suitable for environmental and biological applications (Prasad et al., 2023, 2024). These materials are usually composed of intricate typeset substances and need external mechanical activation. These systems function but

CONTACT Kah-Yoong Chan kychan@mmu.edu.my Faculty of Artificial Intelligence and Engineering, Multimedia University, Persiaran Multimedia, Cyberjaya, Selangor 63100, Malaysia

need engineered synthetic materials and mechanical stimulation. Plant cells generate energy via ionic transport and metabolic processes. This reduces mechanical activation and vibration. The plant-based cells (PBCs) generate very little energy, making them suitable for monitoring agricultural environments (Rahman, Eng, et al., 2025). This difference highlights the special and unique position of plant-based systems within the overall scheme of renewable energy systems.

Plant-based energy harvesting, in comparison with other well-established forms of renewable energy sources, such as solar, wind, hydro, and bioenergy, is a relatively underexplored area of energy harvesting, although its potential is considerable. These systems are carbon-neutral and can easily be incorporated into a natural ecosystem without causing structural or ecological disruption. They also enable low-power solutions for distributed applications, such as precision agriculture, remote environmental monitoring, and Internet of Things (IoT) networks that can operate at the edge of infrastructure availability or in the absence of traditional infrastructure, in particular, where infrastructure is scant (Singh, 2022).

Recent developments in the field of ambient energy harvesting have underscored the need for soft bio-integrated systems that are designed to work in natural environments. New technologies such as self-powered wound healing materials, nanoscale ambient energy harvesters for distributed sensors, and hydrogel-based ionic energy systems have incorporated the concepts of biocompatibility with energy harvesting capabilities in soft materials (Cao et al., 2025; Gao et al., 2024; Gong et al., 2025). The study has indicated the development of sustainable energy technologies with reduced power consumption in natural systems where electrochemical energy harvesting in plants is possible.

One of the revolutionary innovations in this field is the PBC, in which metal electrodes are introduced into plant tissues (roots, leaves, or stems) to harvest electricity from natural biochemical processes. The exploited mechanisms include ion currents related to water conduction through phloem and xylem in the plant, as well as respiration and photosynthesis (Guesmi et al., 2022). It is reported that PBCs can generate 3.877 mW and have been suggested for usage in *Aloe vera* and *Bryophyllum pinnatum* (Chong et al., 2019; Rahman, Eng, et al., 2025). PBCs are fundamentally different from microbial fuel cells in that they rely on direct electron transfer at the plant – electrode interface rather than mediated electron transfer. This approach simplifies system architecture and enables energy harvesting in real time (Lajis et al., 2021).

The shift to plant-based energy systems in a circular bioeconomy context is more effective when the plant is used for more than just energy production or carbon storage. In series-parallel, the prickly pear (*Opuntia ficus-indica*) biobattery based on copper and zinc electrodes powers IoT devices for agriculture (Bouallegue et al., 2025). Bioelectrochemical systems (BES) offer a promising approach to energizing wireless sensors observing crucial agricultural parameters by harvesting waste bioenergy, which in turn aids in ensuring sustainable agriculture (Li et al., 2015). Studies on biocompatible electrodes and energy-efficient systems are progressing, indicating that plant power harvesting could be a viable option for supplementing conventional renewable energy sources in environmentally sensitive areas to power the growing number of IoT devices in agriculture and animal husbandry (Ting & Chan, 2024).

Plant-based energy harvesting systems face a critical limitation: conventional metal electrodes, such as zinc (*Zn*) and copper (*Cu*), release cytotoxic ions that can trigger chlorophyll degradation and foliar necrosis within weeks (Muhammad et al., 2021; Riyazuddin et al., 2022). Polymer-based coatings can mitigate the ion diffusion, but they degrade the electrical performance since the electrode resistance may rise by two or more orders of magnitude (Daniel & Fotheringham, 2007). Graphite coatings offer a somewhat more equitable solution. Due to their impermeable layered nanostructure (interlayer spacing <0.34 nm) and superior electrochemical stability, they can suppress ion leakage by >90% (Jiang et al., 2024), without sacrificing or even enhancing electrochemical performance, with resistance increases usually kept below 20% (Wang et al., 2022). Here, we couple a plant-compatible bio-sealant with graphite-coated electrodes to minimize ion leakage while maintaining good plant health and steady electrical output.

This work extends our previous study (Rahman et al., 2025), in which the electrode distance, material pairing, and diurnal effects were optimized for *Aloe vera*-based PBCs. This current work aims at the enhancement of long-term durability by using graphite-coated electrodes and investigates the biocompatibility of the system and the plant stability in continuous operation. The use of a plant-safe wound healing agent is incorporated in the study in an attempt to minimize the damage to the tissues and, at the same time, ensure a better plant–electrode interface.

2. Materials and methods

In this work, energy harvesting from *Aloe vera* leaves with graphite-coated as well as uncoated metal (*Zn–Cu*) electrodes is studied, and the effects of wound healing agents on leaf vitality and sustainability are also evaluated.

2.1. Experimental overview

The investigation was performed in one stage, named the Sustainability Phase (SP). This stage evaluated the electrical energy and physiological effects for the longer term of the coated and uncoated electrodes using a standardized electrode design. The objective was to evaluate the durability of the system over time in terms of output stability and plant vigour.

2.2. Plant selection and preparation

The experiment was conducted on the high-water-content (~98%) plant, *Aloe vera*, and mature leaves were used, considering the thickness of the fleshy leaves for ease of insertion of the electrode, as well as to prevent loss of moisture. The plant was potted and kept on a home balcony, which allowed us to control the environment as presented in our previous work (Rahman et al., 2025). The plant's growth was followed with great care so that the plant could, without interruptions, be subjected to photoperiods of natural sunlight with minimal direct structural shading from the building. A total of two healthy leaves with a length of 26 cm were employed as the experimental substrate for the entire duration.

For consistency, the same position in the plant cluster was sampled, and at that position, only healthy, nonsenescent whole leaves of the similarly sized and shaped leaves were taken. Aged or wilted leaves were not used to minimize physiological differences between the experiments.

Soil pH was monitored intermittently with initial pH values around 6, as shown in Figure 1(b), indicating a mildly acidic peculiarity, which is typically normalized for *Aloe vera*. The soil was kept consistently moist throughout the time of the experiments to provide a favourable condition for plant growth and the conduction. To ensure an unobstructed electrical response, the soil was not treated with any chemical fertilizers or treatments.

2.3. Electrode design and coating procedure

Zn–Cu electrodes were chosen for the sustainability test based on previous setups. The shapes of all electrode are rectangular with a size of 1.5 cm × 1.25 cm, as shown in Figure 1. *Zn–Cu* electrodes were used both uncoated and coated with graphite.

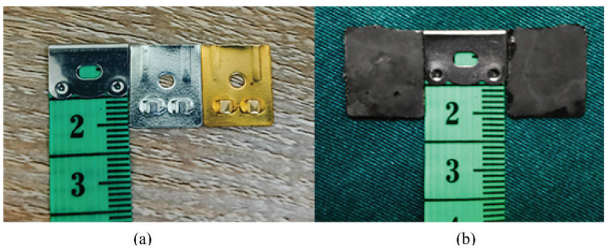

Figure 1. (a) Noncoated *Zn-Cu* electrodes. (b) Coated *Zn-Cu* electrodes.

The graphite-coated electrodes were prepared via a brushing method. The composition of the coating was a mixture of epoxy resin, hardener, and graphite powder with a ratio of 2:1:4, resulting in a medium-thickness coating. The electrodes were cured at room temperature for 10–12 h.

A 2:1 ratio of resin to hardener was used to let the epoxy cure well and stick tightly to the surface of the metal (Yamamoto et al., 2025). The graphite content was raised in order to maintain electrical conductivity within the layer (Bershtein et al., 2002). This balance between mechanical stability and conductivity supports consistent voltage output over the 7-day operation period.

2.3.1. Surface morphology and elemental analysis

To study the surface morphology of coated electrodes, *Cu* and *Zn* samples were, respectively, analyzed by field-emission scanning electron microscopy (FESEM) and energy-dispersive X-ray spectroscopy (EDS) before insertion in plant. Three images were taken from each electrode, from three different positions on the top surface, to check if the coating was uniform. Since the three positions exhibit similar morphologies, a typical image from the middle position is shown in Figures 2 and 3

At 500×, the copper electrode is entirely covered by the composite layer. No large cracks or exposed metal areas can be observed in the scanned area. At 2000× magnification, the surface exhibits a heterogeneous

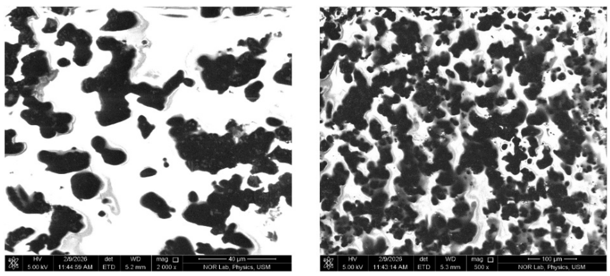

Figure 2. FESEM images of graphite – epoxy coated *Cu* electrode at 2000× and 500× magnifications (top middle).

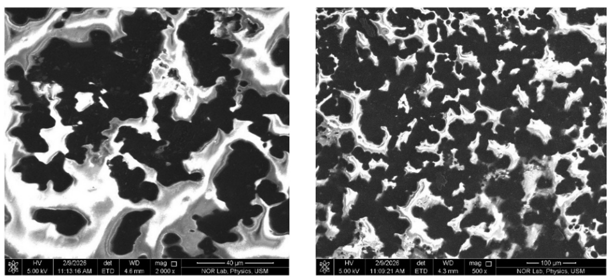

Figure 3. FESEM images of graphite–epoxy coated *Zn* electrode at 2000× and 500× magnifications (top middle).

structure, where darker graphite-rich regions are surrounded by a lighter polymer matrix. The appearance is the same as for a hand-brushed graphite – epoxy layer. While micro-pores and interconnected features may be discerned, the coverage as a whole remains uniform, as shown in Figure 2.

The same surface morphology was observed for the zinc electrode. The zinc displays similar graphite-rich agglomerates separated by polymer-rich boundaries. Differences in pore density and domain sizes are observed, which is to be expected from a manual application of the coating. Apart from these local differences, the surface is macroscopically covered, and no substantial delamination takes place (see Figure 3).

The EDS was performed at the same surface position for the elemental analysis as FESEM. On both electrodes, the outer surface is carbon-rich, as evidenced in Figures 4 and 5. The carbon content for copper is about 83.95 to 85.77 wt%, and the content of oxygen is from 12.58 to 14.15 wt%. A single line of copper (0.15 wt%) was detected at the M site, and none at the L and R sites, see Table 1.

The zinc sample has a carbon range of 84.95 to 86.08 wt% and an oxygen range of 12.59 to 13.39 wt %. There are two points that indicate an extremely small amount of zinc (0.08 and 0.26 wt%), and one point (M) that does not contain zinc, according to Table 2.

The high carbon content implies that the surface is entirely graphite. The oxygen signal originates mainly from the epoxy resin/hardener mixture. Materials based on epoxy contain oxygen-containing functional groups like ether and hydroxyl linkages that are formed during curing, hence a contribution of oxygen from the epoxy system in EDS analysis is expected (Daniel & Fotheringham, 2007). The epoxy oxygen is not from the surface oxidation of the metal substrate.

The very low copper and zinc signals indicate that the metal substrates are still largely covered by the composite layer. The limited exposure of the substrate at isolated locations is indicative of thin regions in the coating where the electron beam interaction volume crosses the substrate (Jiang et al., 2024).

Not conducting EDS characterization after the 7-day plant experiment is a limitation of this study, which is acknowledged. Future studies will include EDS and SEM analysis after exposure to evaluate coating integrity during prolonged bioelectrochemical operation.

Using a digital calliper, coating thickness was calculated at multiple locations over the surface of each electrode. According to the coating thickness measurements, the estimated single-surface coating thickness was 608 µm after the original metal thickness was deducted for zinc and 618 µm for copper. Although some difference was observed across measurement locations, all measurements were within a similar

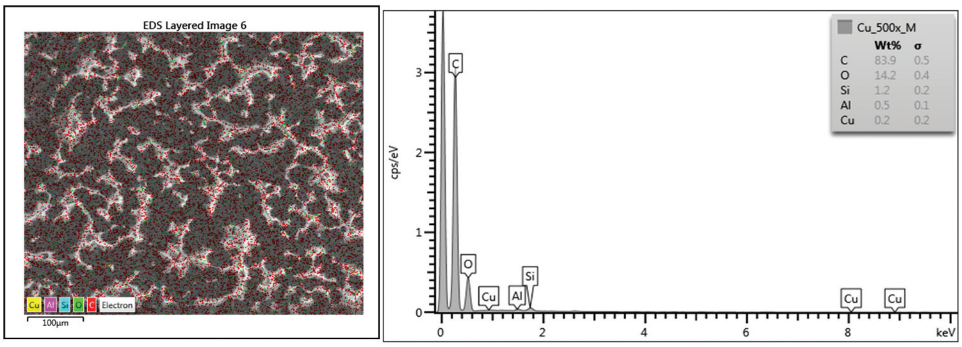

Figure 4. Elemental mapping (left) and representative EDS spectrum (right) of graphite-epoxy coated *Cu* electrode (top middle).

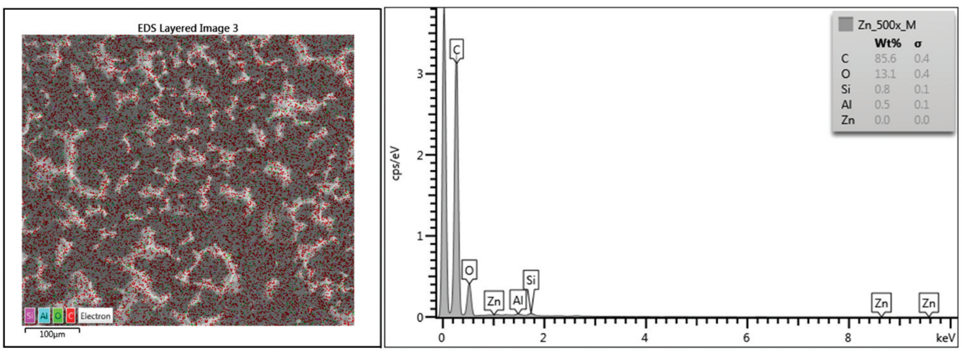

Figure 5. Elemental mapping (left) and representative EDS spectrum (right) of graphite–epoxy coated *Zn* electrode (top middle).

Table 1. EDS (wt%) at left/middle/right (l/m/r) – top of *Cu* Electrode.

Element (wt%)	L	M	R
Al	0.49	0.55	0.53
C	85.77	83.95	84.35
Cu	–	0.15	–
O	12.58	14.15	13.92
Si	1.16	1.20	1.19

Table 2. EDS (wt%) at left/middle/right (L/M/R)-top of *Zn* electrode.

Element (wt%)	L	M	R
Al	0.43	0.48	0.49
C	86.08	85.64	84.95
O	12.59	13.07	13.39
Si	0.83	0.82	0.91
Zn	0.08	–	0.26

range due to the expected hand-brushing variability of the coating.

FESEM and EDS imaging were used to look at surface uniformity, and the same was conducted at three different positions (left, middle, and right). The similar microstructures and high carbon content at the mentioned positions show that the surface is evenly covered, with very little or no metal showing.

Adhesive bonding of the electrode coating was observed during maturation of the coating, during the experiment when electrodes were handled and cleaned with a brush, during a seven-day experiment with plants inserted into the electrodes, and while the electrodes were being inserted into the plant holders. No signs of adhesion failure were visible. Although a formal adhesion test was not performed, the preparation and the subsequent operations of the experiment demonstrated that the coating's adhesion was sufficient.

2.4. Continuous operation with coated and noncoated electrodes

The sustainability testing involved comparing the performance of coated and uncoated *Zn–Cu* electrodes inserted into *Aloe vera* leaves at a fixed distance of 1 cm (optimized from our previous work) (Rahman et al., 2025), and a scale was marked on the leaf to ensure accuracy, as shown in Figure 6.

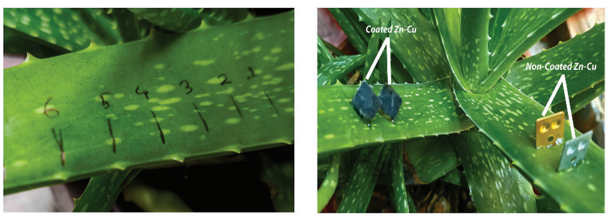

(a) (b)

Figure 6. (a) Scaled leaf. (b) Experimental setup for sustainability testing with coated and noncoated *Zn–Cu* electrode pairs.

Surface cleaning and any contamination were removed by fully wiping the surface of the electrodes with 70% isopropyl alcohol swabs prior to each run. At this point, the electrodes were not withdrawn (after insertion) but left in the same leaf for 7 days. Voltage and current were measured three daily times a day.

To shield the plant tissue from fungal infection or rotting as a result of the extended electrode placement, a plant wound healing substance (anti-bacterial, anti-fungal) was applied at the points of entry.

2.5. Measurement instruments and protocol

The voltage and current were measured by Owon B33 + digital multimeter for 30-min session, 3 times per day at 10:00, 16:00, and 22:00. The ambient temperature and humidity were monitored by Xiaomi Mijia Smart Thermometer 3, while soil moisture, pH, temperature, and light intensity were measured by Avosky Soil Survey Analyzer, as reported in our previous work (Rahman et al., 2025).

The pH was measured to be stable at 6 during the test period. At no point were any outside electrolytes or chemical additives added. The elevated water content of *Aloe vera* gel, along with its inherent ions, sufficed to facilitate the necessary ionic conductivity for operation. The stability of the internal ionic environment of the leaf was attributed to the constant temperature and relative humidity (RH) maintained within a narrow range, leading to a consistent power output of 0.015–0.017 mW in the coated configuration.

The *Zn-Cu* in this work is a galvanic bioelectrochemical cell, which produces power through the spontaneous redox reactions in the ionic plant medium. In the absence of mechanical stimulation due to periodic alternation of polarity, these cells deliver a DC output (Rahman, Eng, et al., 2025). Earlier studies on plant energy harvesting with *Zn–Cu* electrodes demonstrate DC output and assessed performance based on the power relation $P = V \times I$ (Chong et al., 2019). Here, power was also calculated as in the ordinary DC circuit calculation, appropriate for galvanic cells.

3. Results and discussions

In this section, the results of the sustainability evaluation of electric energy harvesting through *Aloe vera* leaves with *Zn–Cu* electrodes are presented. It shows the electrical properties (voltage, current, and power) of graphite-coated and noncoated electrodes during 7-day continuous operation. Trends and deviations are analyzed as a function of electrode surface treatment and plant reaction to controlled environment conditions.

Table 3. Coated vs. noncoated *Zn–Cu* electrodes: voltage, current, power.

Day	*V* (noncoated) (V)	*V* (coated) (V)	*I* (noncoated) (mA)	*I* (coated) (mA)	*P* (noncoated) (mW)	*P* (coated) (mW)
1	0.881	0.663	0.08	0.02	0.069	0.016
2	0.852	0.660	0.10	0.01	0.089	0.017
3	0.894	0.654	0.09	0.02	0.082	0.015
4	0.658	0.671	0.07	0.02	0.069	0.016
5	0.595	0.660	0.05	0.02	0.035	0.016
6	0.456	0.668	0.03	0.02	0.013	0.014
7	0.322	0.669	0.02	0.02	0.009	0.015

3.1. Electrode coating and sustainability plan

In order to evaluate performance and stability of graphite-coated and noncoated *Zn–Cu* electrodes for plant experimental energy harvesting, voltage, current, and power measurements were taken three times a day for a duration of 7 days continuously, as shown in Table 3. Daily averages were computed, and the results are plotted for comparison.

The voltage output of the noncoated *Zn–Cu* electrodes started at a fairly high value (Figure 7), with a mean of 0.881 V for the first day and a maximum value of 0.894 V for Day 3. This was mainly due to the high electrochemical activity of noncoated *Zn* and *Cu* in the *Aloe vera* leaf ionic medium. After Day 3, a drastic voltage fall was observed, dropping to 0.322 V at Day 7, which was ascribed to tissue deterioration, cell necrosis, and reduction of ionic conductivity due to metal ion leakage (Zn^{2+} and Cu^{2+}) (Iyebeye et al., 2025; Wang et al., 2022).

Conversely, in terms of Figure 8, the graphite-coated electrodes exhibited a consistent voltage output of approximately 0.66 V during the experiment, attributable to the inert and biocompatible properties of graphite, which mitigated tissue stress and ion diffusion into the plant (Wang et al., 2022). This confirms the long-term reliability of the coated setup.

These specific stability properties of graphite-coated electrodes can be attributed to both the structural and electrochemical properties of graphite. Graphite is composed of layers of carbon bonded in a sp^2 configuration with an interlayer spacing of 0.335 nanometers. Such a design is sufficiently dense to be effectively impermeable to hydrated metal ions, such as Zn^{2+} and Cu^{2+} (Rozpłoch et al., 2007). Since these metal ions have larger hydrated ionic radii, the layers of graphite act as a physical diffusion barrier to ions moving away from the electrode system. In addition, graphite is electrochemically stable and corrosion-free under gentle aqueous conditions, which can also work to inhibit metal dissolution at the interface of the electrode (Blomquist et al., 2017). Less ion migration means less stress in the system. This is one of the reasons why the current (~0.02 mA) remained steady during 7 days of uninterrupted operation.

At the beginning, noncoated electrodes yielded a large current, reaching a maximum of 0.107 mA at Day 2 as a result of rapid electron transfer at the clean electrode surfaces. However, the current gradually decreased, reaching 0.028 mA at Day 7. This decrease coincides with the decline and drying out of leaves in the infected parts. Nevertheless, the current for the graphite-coated electrodes is lower at the beginning (~0.017 mA), and the stability of the current output is higher in the range of 0.02–0.025 mA. This shows that although the noncoated electrodes have enhanced early performance, the degradation limits the usability.

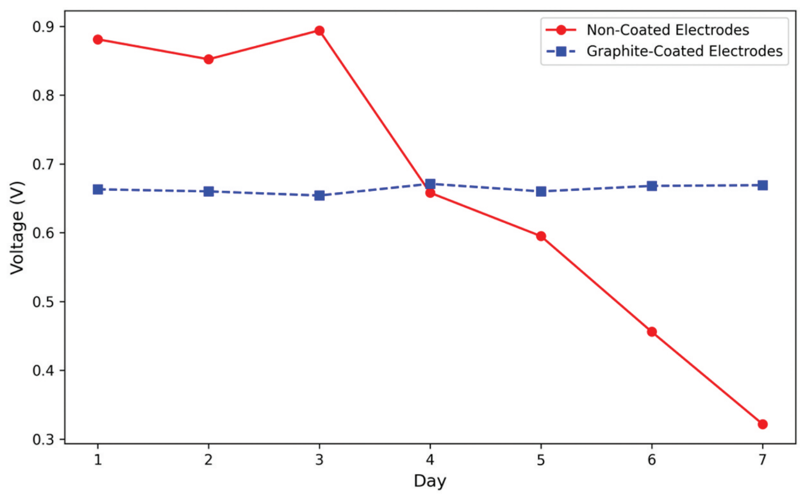

Figure 7. Graph comparing average voltage (*V*) between graphite-coated and noncoated *Zn–Cu* electrodes.

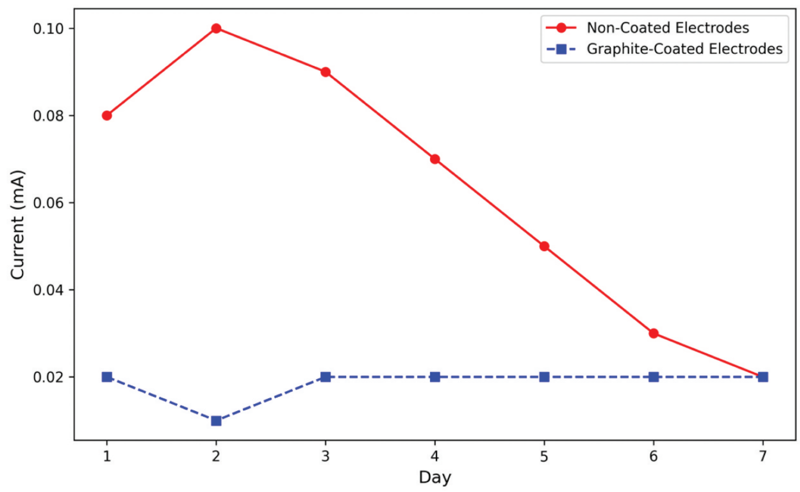

Figure 8. Graph comparing average current (mA) between graphite-coated and noncoated *Zn–Cu* electrodes.

The Power, $P = V \times I$, also showed the same trend. The uncoated version reached a peak of 0.0895 mW on Day 2, but this value dramatically dropped over the next 3 days due to a reduction of conductivity and cell viability in the damaged leaf. The result is that the power was close to constant and equal to ≈0.015–-0.017 mW with negligible oscillations for the system treated with graphite (Figure 9). A steady power source is essential for such applications as low-power IoT devices, which demand long life more than maximum output.

To balance the potential impact of environmental conditions, all parameters were tracked daily, as summarized in Table 4. Soil pH value was measured for a similar period of time (every day for 7 days) and remained relatively constant in an acidic state (pH = 6). Ambient temperature ranged from 26 to 33°C, with mean values around 30°C and humidity levels between 73% and 84%.

Although the environmental parameters displayed slight variations, the multifactor environmental (temperature and humidity) was relatively constant. Post day 3, the bare electrodes demonstrated a consistent decline in electrical output. The fluctuations in electricity production were not associated with variations in environmental temperature and humidity. The decline in electric performance may be attributed to the degradation of the inner tissue of the bare electrodes. The output of the coated electrodes was found to be stable in the same environmental conditions, suggesting stability in the coating of the electrodes.

For the sake of reproducibility and transparency, the entire time-series data are freely available in a public data repository. The repository can be accessed through the DOI provided.

Slight variations in voltage and current were detected during the entire monitoring period. These fluctuations are inherent in plant-based bioelectrochemical systems as a result of the coupling of dynamic biology and electrochemistry (Timmers et al., 2010). Diurnal changes in metabolism and transpiration may affect ionic movement in leaf tissue and could result in short-term fluctuations of the

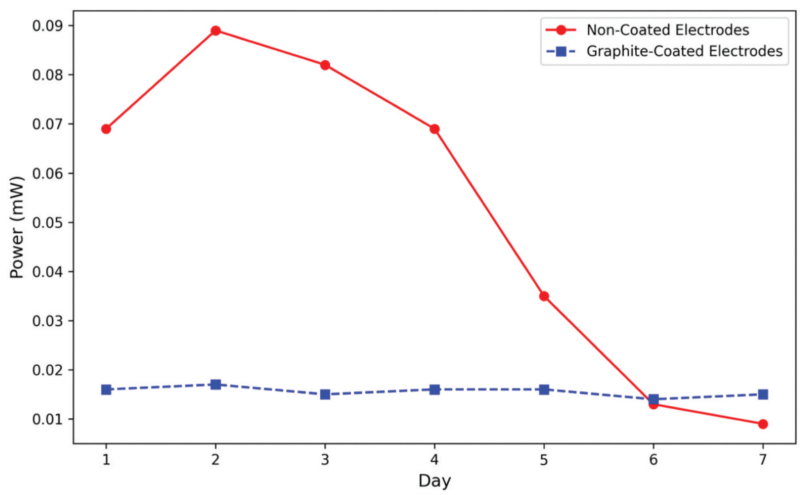

Figure 9. Graph comparing average power (mW) between graphite-coated and noncoated *Zn–Cu* electrodes.

Table 4. Summary of environmental conditions during 7-day monitoring.

Parameter	Range	Average
pH	6	6
Temperature (°C)	26–33	29.9
Humidity (%)	73–84	78.1

measured output (Rahman, Eng, et al., 2025). Furthermore, slow drifts in individual electrolyte resistance and local electrode polarization at the introduction points may induce small drifts over time. Because the ambient temperature and humidity were consistent and stable, the deviations are more likely to be caused by inherent physiological processes rather than by fluctuations in the external environment (Huigen et al., 2002).

Figure 10 represents the trade-off between maximal magnitude and long-term stability. In noncoated electrodes, the output is greater at the start of the first several days, but it rapidly declines as a result of tissue necrosis. The coated electrodes show very minor variations in voltage, current, and power, indicating a stable output as a function of time. This stability is a more equal trade-off between electrical efficiency and biocompatibility, since a lower ionic leakage corresponds to a preserved tissue and a stable internal resistance. Despite slightly reduced peak values, the coated system provides a stable and predictable output, which is more adequate for the low-power IoT and distributed sensing applications. In those cases, the peak transient is typically traded for reliability.

As shown in Figure 11, noncoated *Zn–Cu* plates were employed to evaluate the physical deterioration of an *Aloe vera* leaf for 7 days. Day 1: The leaf looked healthy and unstressed. Electric output climbed initially and reached a maximum at around Day 3. The direct contact of fresh *Zn* and *Cu* surfaces with the ionic plant substrate allows for an active oxidation, generation of charges, and moistening of the inner tissue, fertilizing the tissue, with caused this early acceleration.

Slight discolouration was observed with focal softening near the site of electrode penetration on Day 4, indicating tissue damage. Uncoated electrodes have been shown to invariably release Zn^{2+} and Cu^{2+} ions in the gel matrix. Metal ions are capable of diffusing across cell membranes, where they disrupt the

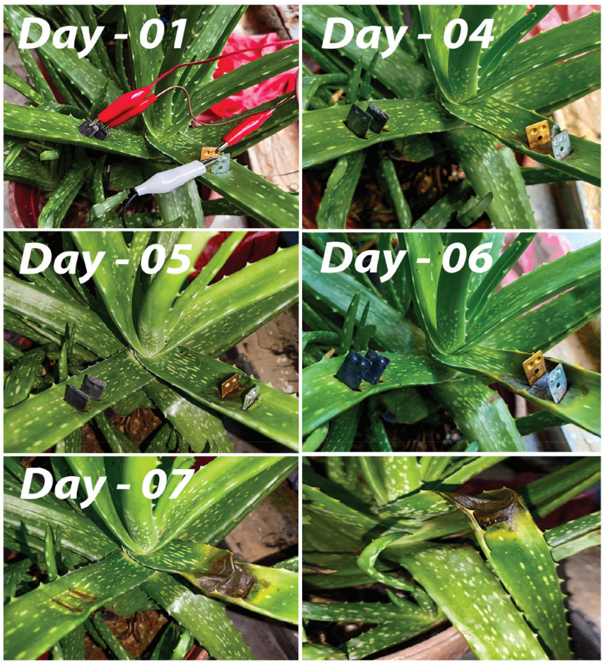

Figure 11. Progressive deterioration of *Aloe vera* leaf subjected to noncoated *Zn–Cu* electrodes over 7 days.

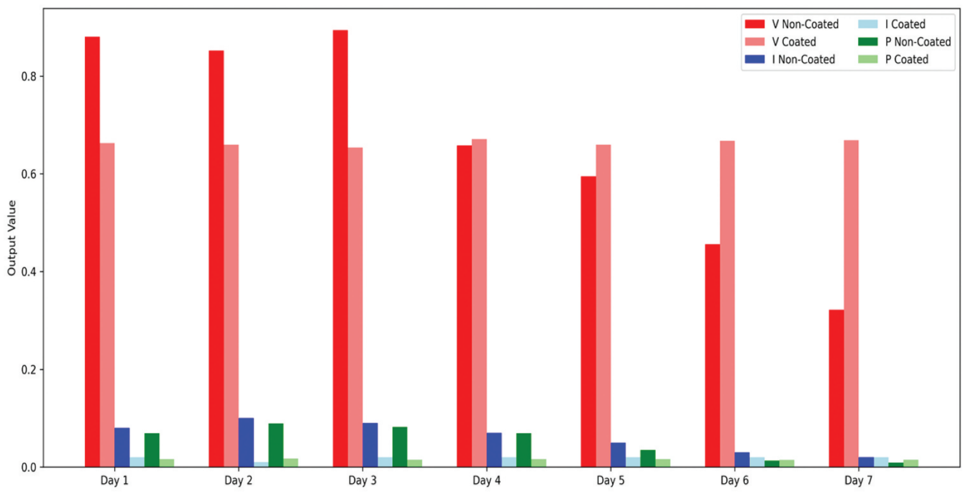

Figure 10. Voltage, current, and power output of graphite-coated vs. noncoated *Zn–Cu* electrodes.

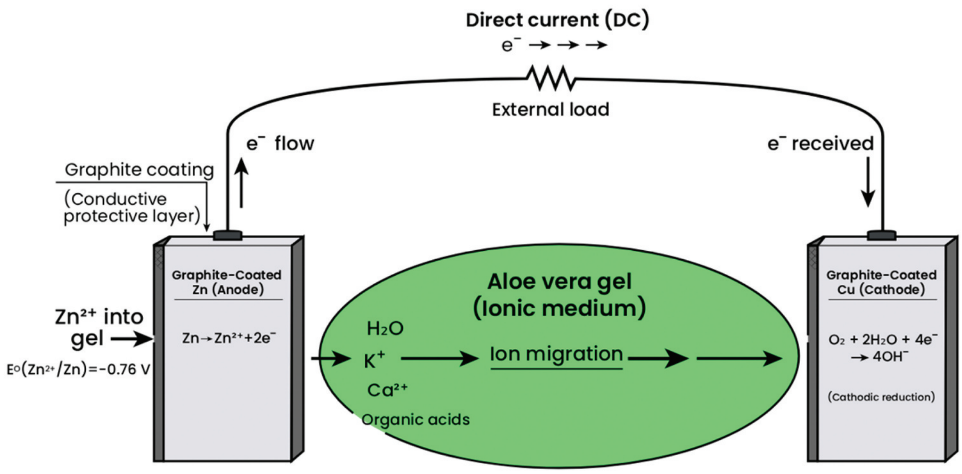

Figure 12. Schematic illustration of the proposed bioelectrochemical mechanism in the Gr-coated *Zn–Cu Aloe vera* system.

membranes and osmotic balance of the cells, and ultimately the turgor of the cells. On Day 5 and 6, leaf wilting associated with necrotic lesions was observed as an indication of leaf physiological stress.

By Day 7, the leaf was wilted, partially collapsed, liquefied intercellularly and desiccated. As the tissue is dehydrated, cell membranes lose integrity, and the fall in turgor pressure reduces the ionic mobility within the gel-like cytoplasm. This dehydration, along with the sustained leakage of metal ions from the unprotected electrodes, led to an increase in the internal resistance and a reduction of the charge transport within the electrodes (Zou et al., 2021). A rise in resistance is responsible for the drop in voltage from the maximum observed on Day 3 (0.894 V) to 0.322 V on Day 7. The visual breakdown of Figure 12 reveals the lack of stability of the electrochemistry of the non-coated design and indicates how loss of cell function and moisture results in the decline in performance over time.

This investigation demonstrates a steady monitoring performance for 7 days under ambient conditions. However, since this period also implies stability of the performance, long-term monitoring is required to assess the long-term sustainability.

3.2. Proposed electrochemical mechanism

The *Zn–Cu* pair embedded inside the *Aloe vera* tissue behaves as a bio-assisted galvanic cell. It is the spontaneous redox reaction between the metal surface and electrolyte within the plant tissue that produces the voltage. Due to this, Zn^{2+}/Zn (−0.76 V) has a lower standard electrode potential ($E°$) than Cu^{2+}/Cu (0.34 V), so zinc gets oxidized to form Zn^{2+} ions by the reaction $Zn \rightarrow Zn^{2+} + 2e^{-}$ (Rahman, Eng, et al., 2025).

The electrons released are responsible for the flow of DC to the copper electrode through the external circuit. In the aqueous *Aloe vera* gel, the copper electrode experiences the cathodic reaction where the dissolved oxygen is reduced. At mildly acidic to near-neutral conditions (pH ≈ 6), the dominant reaction at the cathode is $O_2 + 2\,H_2O + 4e^{-} \rightarrow 4OH^{-}$ (Rahman, Eng, et al., 2025).

The internal electrolyte of the galvanic cell is the *Aloe vera* gel. The high-water content of the gel contains organic acids and the naturally occurring ions like K^{+}, Ca^{2+} , etc., which facilitate the gel's function by making ionic transport possible (Rahman, Eng, et al., 2025). It is because of this ionic migration that electro-neutrality is maintained between the electrodes, thus completing the electrochemical circuit. For this reason, the system is a combination of a classical galvanic cell and a biological matrix that is in agreement with electrochemical principles, as demonstrated in Figure 12 (Aikens, 1983; Chong et al., 2019; Logan et al., 2006).

The graphite coating changes the metal–electrolyte interface in two significant ways. It offers a conductive pathway that promotes effective electron transfer. It also serves as an interfacial protective layer that diminishes the amount of direct exposure of *Zn* and *Cu* to the biological medium. By restricting the rapid dissolution of metal ions, the coating lessens the injury to the surrounding tissue and slows the degradation of the electrode. This stabilization of the interface accounts for the improved consistency of output and reduced necrosis seen in electrodes that were coated.

3.3. Evaluation of plant wound-healing agent on leaf longevity

A commercially available plant wound healing agent was applied after each diagnostic cycle to mitigate physiological stress and reduce the risk of microbial infections at the electrodes' insertion sites (Figure 13). The agent established a temporary protective barrier on the skin surfaces by reducing moisture loss and inhibiting bacterial and/or fungal proliferation. The protective effect is constrained

Figure 13. Application of wound-healing agent to *Aloe vera* leaf.

due to the agent being diluted and diffused within the aqueous, ion-rich *Aloe Vera* gel. The agent was shown to delay external decay; however, it did not mitigate the ongoing electrochemical ion loss from the electrodes or the decomposition of internal tissues. Eventually, even outer layers were affected by softening, localized breakdown, and shrivelling. This indicates that the gel acted only as a transient barrier and not as a protective agent.

4. Conclusion

This work focused on investigating the durability and cytocompatibility of uncoated and coated *Zn–Cu* electrodes in *Aloe vera* leaves by applying effective energy extraction under real conditions. Coated electrodes provided much better stability of output and less degradation of plant material than uncoated electrodes during an extended period of 7 days. Uncoated electrodes showed higher initial voltage and current, but their performance dropped significantly as a result of expected ion leakage and tissue necrosis. Conversely, the graphite-coated electrodes demonstrated stable electrical performance with less physiological damage, indicating potential for long-term use in bioenergy devices. Our results indicate that inert and plant-compatible electrode designs can be used to enable stable, maintenance-free energy delivery for potential use in smart agriculture and environmental sensing in remote locations. General environmental factors such as sunlight and moisture were observed; however, complete control of the climate was not possible because of the semi-outdoor setup. In the next work, the long-term stability, biocompatibility, and power output at continuous operation of the electrodes will be addressed for 30 days.

Disclosure statement

No potential conflict of interest was reported by the author(s).

ORCID

Kah-Yoong Chan http://orcid.org/0000-0003-1076-5034

Data availability statement

All datasets used to support the conclusions of this article are available from the public data repository at the website of https://doi.org/10.5281/zenodo.18756280.

References

Aikens, D. A. (1983, January). Electrochemical methods, fundamentals and applications. *Journal of Chemical Education*, *60*(1), A25. https://doi.org/10.1021/ed060pA25.1

Bershtein, V. A., Egorova, L. M., Yakushev, P. N., Pissis, P., Sysel, P., & Brozova, L. (2002, May). Conductive mechanism of polymer/graphite conducting composites with low percolation threshold. *Journal of Polymer Science, Part B, Polymer Physics*, *40*(10), 954–963. https://doi.org/10.1002/polb.10141

Blomquist, N., Wells, T., Andres, B., Bäckström, J., Forsberg, S., & Olin, H. (2017, January). Metal-free supercapacitor with aqueous electrolyte and low-cost carbon materials. *Scientific Reports*, *7*(1), 39836. https://doi.org/10.1038/srep39836

Bouallegue, B., Guesmi, H., Ayachi, C., & Ajjel, R. (2025). Sustainable energy solutions: Leveraging prickly pear biobatteries and efficient software for IoT in agriculture. *Energy Reports*, *14*, 5388–5400. https://doi.org/10.2139/ssrn.5199273

Cao, J., Dong, J., Wu, J., & Suwardi, A. (2025, July 11). Evapolectrics: Direct harvesting of electricity from evaporation using thermoelectrics. *ACS Nano*, *19*(28), 26249–26258. https://doi.org/10.1021/acsnano.5c10693

Cherp, A., Vinichenko, V., Tosun, J., & Gordon, J. A., Jewell, J. (2021, July). National growth dynamics of wind and solar power compared to the growth required for global climate targets. *Nature Energy*, *6*(7), 742–754. https://doi.org/10.1038/s41560-021-00863-0

Chong, P. L., Singh, A. K., & Kok, S. L. (2019, December). Potential application of aloe vera-derived plant-based cell in powering wireless device for remote sensor activation. *PLOS ONE*, *14*(12). https://doi.org/10.1371/journal.pone.0227153

Choong, F. C. M., & May, Y. Y. (2023, September). Journal of engineering technology and applied physics an improved DC-DC boost converter for energy harvesting. *Journal of Engineering Technology and Applied Physics*, *5*(2), 69–78. https://doi.org/10.33093/jetap.2023.5.2

Daniel, A., & Fotheringham, A. (2007, April). Microstructured conducting polymer coatings on plastic strip for contact electrodes: Formulation and tuning of sheet resistance. *Journal of Applied Polymer Science*, *104*(1), 234–237. https://doi.org/10.1002/APP.25556

Feng, Y., Zhang, L., Zheng, Y., Wang, D., Zhou, F., & Liu, W. (2019, January). Leaves based triboelectric nanogenerator (TENG) and TENG tree for wind energy harvesting. *Nano Energy*, *55*, 260–268. https://doi.org/10.1016/j.nanoen.2018.10.075

Gao, S., Rao, Y., Wang, X., He, Q., Yang, M., Wang, Y., Zhou, Y., Guo, J., & Yan, F. (2024). Skin temperature-activated multifunctional thermoelectric dressing for bacterial infected wound treatment. *Advanced Functional Materials*, *35*(6). https://doi.org/10.1002/adfm.202415085

Gitelman, L. D., & Kozhevnikov, M. V. (2023, March). New approaches to the concept of energy transition in the times of energy crisis. *Sustainability*, *15*(6), 5167. https://doi.org/10.3390/su15065167

Gong, Z., Suwardi, A., & Cao, J. (2025, April 7). Electricity generation from ambient water evaporation in the absence of sunlight via PVA-based porous hydrogels. *Advanced Functional Materials*, *36*(6). https://doi.org/10.1002/adfm.202423371

Guesmi, H., Ajjel, R., Alqahtani, T., & Algarni, S. (2022). Towards renewable green energy produced by prickly pear living plant. *International Journal of Sustainable Engineering*, *15*(1), 253–265. https://doi.org/10.1080/19397038.2022.2140223

Haegel, N. M., Atwater, H., Barnes, T., Breyer, C., Burrell, A., Chiang, Y.-M., De Wolf, S., Dimmler, B., Feldman, D., Glunz, S., Goldschmidt, J. C., Hochschild, D., Inzunza, R., Kaizuka, I., Kroposki, B., Kurtz, S., Leu, S., Margolis, R., Matsubara, K. ... Yamaguchi, M. (2019). Terawatt-scale photovoltaics: Transform global energy, improving costs and scale reflect looming opportunities. *Science*, *364*(6443), 836–838. https://doi.org/10.1126/science.aaw1845

Huigen, E., Peper, A., & Grimbergen, C. A. (2002). Investigation into the origin of the noise of surface electrodes. *Medical and Biological Engineering and Computing*, *40*(3), 332–338. https://doi.org/10.1007/BF02344216

Intergovernmental Panel on Climate Change. (2023). *Climate change 2021 - the physical science basis*. Cambridge University Press. https://doi.org/10.1017/9781009157896

Iyebeye, K. O., Samuel-Ekpe, N. I., Ekwedigwe, C. M., & Nwambu, C. N. (2025). High-performance graphite-reinforced sustainable epoxy composite. *Open Journal of Chemistry*, *11*(1), 009–013. https://doi.org/10.17352/ojc.000044

Jacobson, M. Z., Delucchi, M. A., Cameron, M. A., Coughlin, S. J., Hay, C. A., Manogaran, I. P., Shu, Y., & von Krauland, A.-K. (2019, December). Impacts of Green New Deal energy plans on grid stability, costs, jobs, health, and climate in 143 countries. *One Earth*, *1*(4), 449–463. https://doi.org/10.1016/j.oneear.2019.12.003

Jiang, Z., Wei, J., Li, H., Chen, R., Yang, W., Ma, G., Nishimura, K., Guo, P., & Wang, A. (2024, April). Enhanced corrosion resistance of graphite-like carbon coatings via dense ta-C interlayer encapsulating. *Diamond and Related Materials*, *142*, 111139. https://doi.org/10.1016/j.diamond.2024.111139.C

Lajis, G. A., Jasni, J., Azis, N., Radzi, M. A. M., Mohtar, M. N., & Salim, N. A. (2021, March). Bioelectricity harvesting at aquaponics system: Current and future challenges. In *2021 IEEE International Conference in Power Engineering Application (ICPEA)* (pp. 85–90). IEEE. https://doi.org/10.1109/ICPEA51500.2021.9417840

Li, X., Abu-Reesh, I. M., & He, Z. (2015, September). Development of bioelectrochemical systems to promote sustainable agriculture. *Agriculture*, *5*(3), 367–388. https://doi.org/10.3390/agriculture5030367

Logan, B. E., Hamelers, B., Rozendal, R., Schröder, U., Keller, J., Freguia, S., Aelterman, P., Verstraete, W., & Rabaey, K. (2006, September). Microbial fuel cells: Methodology and technology. *Environmental Science and Technology*, *40*(17), 5181–5192. https://doi.org/10.1021/es0605016

Muhammad, I., Shalmani, A., Ali, M., Yang, Q. H., Ahmad, H., & Li, F. B. (2021, January). Mechanisms regulating the dynamics of photosynthesis under abiotic stresses. *Frontiers in Plant Science*, *11*. https://doi.org/10.3389/fpls.2020.615942

Prasad, G., Woo, I., Yoon, J. U., & Bae, J. W. (2024, January). Synergetic effects of amino-functionalized reduced graphene oxide and barium strontium titanate pillars on enhancing triboelectric performance. *Advanced Sustainable System*, *8*(1), 2300385. https://doi.org/10.1002/adsu.202300385

Prasad, G., Yoon, J. U., Woo, I., & Bae, J. W. (2023, August). Fabrication of amino and fluorine functionalized graphene-based polymer composites to enhance the electromechanical conversion efficiency of TENGs for energy-harvesting applications. *Chemical Engineering Journal*, *470*, 144280. https://doi.org/10.1016/j.cej.2023.144280

Rahman, S. R. (2025). Energy harvesting from plants using plant-based cells. In *2025 Multimedia University Engineering Conference (MECON)*, IEEE, Cyberjaya, Malaysia. https://doi.org/10.1109/MECON67253.2025.11277229

Rahman, S. R., Eng, N. E., Ashraf, M. A., Pang, W.-L., Tan, K. B., Singh, A. K., & Chan, K.-Y. (2025, December). Energy harvesting from living plant: A review on past research and way forward. *Energy Reports*, *14*, 268–281. https://doi.org/10.1016/j.egyr.2025.06.021

Riyazuddin, R., Nisha, N., Ejaz, B., Khan, M. I. R., Kumar, M., Ramteke, P. W., & Gupta, R. (2022, January). A comprehensive review on the heavy metal toxicity and sequestration in plants. *Biomolecules*, *12*(1), 43. https://doi.org/10.3390/biom12010043

Rozpłoch, F., Patyk, J., & Stankowski, J. (2007). Graphenes bonding forces in graphite. *Acta Physica Polonica A*, *112*(3), 557–562. https://doi.org/10.12693/APhysPolA.112.557

Shukor, N. I. A., Chan, K.-Y., Thien, G. S. H., Yeoh, M.-E., Low, P.-L., Devaraj, N. K., Ng, Z.-N., & Yap, B. K. (2023, October). A green approach to natural dyes in dye-sensitized solar cells. *Sensors*, *23*(20), 8412. https://doi.org/10.3390/s23208412

Singh, A. K. (2022). Plant base renewable energy to power nanoscale sensors. In B. Dudem, V. Venkateswaran, & A. Chandrasekhar (Eds.), *Nanogenerators and self-powered systems*. IntechOpen. (pp. 1–12). https://doi.org/10.5772/intechopen.105365

Stritzke, S., & Jain, P. (2021, July). The sustainability of decentralised renewable energy projects in developing countries: Learning lessons from Zambia. *Energies*, *14*(13), 3757. https://doi.org/10.3390/en14133757

Tan, J. Y., & Chan, K. Y. (2024, December). Solar-based nighttime electric power generator based on radiative cooling. *Energy Reports*, *12*, 5155–5162. https://doi.org/10.1016/j.egyr.2024.11.024

Timmers, R. A., Strik, D. P. B. T. B., Hamelers, H. V. M., & Buisman, C. J. N. (2010). Long-term performance of a plant microbial fuel cell with Spartina anglica. *Applied Microbiology and Biotechnology*, *86*(3), 973–981. https://doi.org/10.1007/s00253-010-2440-7

Ting, Y. T., & Chan, K. Y. (2024, June). Optimising performances of LoRa based IoT enabled wireless sensor network for smart agriculture. *Journal of Agriculture and Food Research*, *16*, 101093. https://doi.org/10.1016/j.jafr.2024.101093

Victoria, M. (2021). Solar photovoltaics is ready to power a sustainable future. *Cell Press.* , 2021. https://doi.org/10.1016/j.joule.2021.03.005

Wang, K. L., Yang, H., Yu, S., Jiang, K., & Jiang, K. (2022, August). Electrochemical behavior of Cu-mediated electrowinning-coupled CO2 capture. *Electrochimica Acta*, *422*, 140571. https://doi.org/10.1016/j.electacta.2022.140571

Yamamoto, S., Phan, N. T., Kihara, K., Shundo, A., & Tanaka, K. (2025, April). Off-stoichiometry effect on the physical properties of epoxy resins. *Polymer Journal*, *57*(4), 357–366. https://doi.org/10.1038/s41428-024-00983-w

Yeoh, M. E., & Chan, K. Y. (2017, December). Recent advances in photo-anode for dye-sensitized solar cells: A review. *International Journal of Energy Research*, *41* (15), 2446–2467. https://doi.org/10.1002/er.3764

Yeoh, M. E., & Chan, K. Y. (2021, March). A review on semitransparent solar cells for real-life applications based on dye-sensitized technology. *IEEE Journal of Photovoltaics*, *11*(2), 354–361. https://doi.org/10.1109/JPHOTOV.2020.3047199

Zou, F. (2021, December). Long-life $LiNi0.5Mn1.5O4$/graphite lithium-ion cells with an artificial graphite-electrolyte interface. *Energy Storage Materials*, *43*, 499–508. https://doi.org/10.1016/j.ensm.2021.09.033